MICROPARTICLE MANIPULATION BY A FOUR-SPIRAL ELECTRODE MICROSTRUCTURE

MANIPULACIÓN DE MICROPARTÍCULAS POR MEDIO DE UNA MICROESTRUCTURA DE ELECTRODOS EN ESPIRAL

Flavio Humberto Fernández Morales*
Julio Enrique Duarte**
Joseph Samitier Marti***

Resumen

En el presente artículo se describe el funcionamiento de una microestructura compuesta por cuatro electrodos en espiral, desarrollada en tecnología CMOS, que fue diseñada para obtener el movimiento lineal de micropartículas. Este dispositivo utiliza el fenómeno de dielectroforésis de onda viajera (TWD) como principio de funcionamiento, y es afectado por los efectos electrohidrodinámicos (EHD). Para determinar el comportamiento de las partículas se efectuaron cálculos numéricos por el método de los elementos finitos. Con el fin de probar el microsistema se utilizaron microesferas de poliestireno de 6 m de diámetro.

Abstrac

The focus of attention of this paper is to explain the operation of a four-spiral electrode microstructure, wholly developed in CMOS technology, that has been designed to achieve linear motion of microparticles. This device makes good use of the travelling wave dielectrophoresis (TWD) phenomenon and is affected by the electrohydrodynamic (EHD) effects. Numerical simulations were carried out by means of the Finite Element Method to assess the particle behaviour. The microsystem was tested employing polystyrene microspheres of 6 m in diameter.

KEY WORDS

Computer modelling and simulation of medical and biological techniques, Micromanipulators, Electrohydrodynamics

** Ingeniero electrónico, Universidad Distrital Francisco José de Caldas. Ph.D., en Ingeniería Electrónica, Universidad de Barcelona, España. Profesor asociado, Universidad Pedagógica y Tecnológica de Colombia Facultad Seccional Duitama. Grupo de Energía y Aplicación de Nuevas Tecnologías GEANT. E-mail: flaviofm1@gmail.com.*

***Licenciado en Física, Universidad Industrial de Santander. Ph.D., en Física, Universidad de Barcelona, España. Profesor titular, Universidad Pedagógica y*
Tecnológica de Colombia Facultad Seccional Duitama, Grupo de Energía y Aplicación de Nuevas Tecnologías GEANT. E-mail: julioenriqueduarte@latinmail.com

****Ph.D., en Física, Universidad de Barcelona, España. Profesor Catedrático, Departamento de Electrónica, Universidad de Barcelona, España. samitier@el.ub.es*

1. INTRODUCTION

Nowadays the development of bioparticle-microhandling microtools is one of the most important and active research fields in order to provide biomedical, biological and pharmacological researchers with adequate devices to perform handling of biological material (Figeys and Pinto, 2000; Hughes, 2003). In this way a well-accepted technique is one which employs electric fields like mechanism of actuation (Fuhr et al., 1992). Travelling wave dielectrophoresis (TWD) is a technique based on common dielectrophoresis (cDEP), i.e. it is based on the motion of electrically neutral matter caused by its interaction with non-uniform electric fields (Pohl, 1951). When the electrode shapes and their polarisation voltages are suitable, they can generate travelling-wave electric fields that induce microparticle motion (Goater, 1997)

In general, it is a common practice to design microparticle conveyors as periodical structures based upon a pattern of n square or sinusoidal phases shifted $360^o/n$ from each other (Hughes et al., 1994).

In this paper it is shown a microsystem designed to achieve linear motion of biological objects. Figure 1. shows the tested microstructure, which was wholly developed in CMOS technology. The microsystem consists of an arrangement of four-spiral square-bipolar-driven electrodes and was tested using polystyrene microspheres of 6 μm in diameter. In the sequel, numerical and experimental results are outlined.

2. THEORETICAL BACKGROUND

As shown in Figure. 2, forces exerted on a particle placed over the central part of the spiral arms are given by:

$$\mathbf{F}_{\mathrm{DEP}} = \mathbf{F}_{\mathrm{G}} \quad (1)$$

$$\mathbf{F}_{\mathrm{TWD}} = \mathbf{F}_{\mathrm{v}} \quad (2)$$

Where the dielectrophoretic force $\mathbf{F}_{\mathrm{DEP}}$, see equation 3 (Pohl, 1978), is responsible for carrying the particle to a stable levitation height counteracting the sedimentation force $\mathbf{F}_{\mathrm{G}}$ due to the gravity action, see equation 4.

$$\mathbf{F}_{\mathrm{DEP}} = 2\,\pi\,\varepsilon_0\,\varepsilon_m\,r^3\,\mathrm{Re}[\mathrm{F_{CM}}]\nabla\left|\mathbf{E}\right|^2 \quad (3)$$

where $\varepsilon_0 = 8.854\text{x}10^{-12}$ (Farad m^{-1}) is the free-space permittivity, ε_m is the relative medium dielectric permittivity, r is the radius of a spherical particle, $\mathrm{Re}[F_{CM}]$ is the real part of the Clausius-Mosotti factor, see equation 5 (Talary et al., 1996), $\mathbf{E}$ is the strength of the electric field and ∇ is the gradient vector operator.

$$\mathbf{F}_G = \frac{4\pi r^3}{3}(d_2 - d_1)\mathbf{g} \quad (4)$$

where $\mathbf{g}$ is the acceleration due to gravity, d_1 and d_2 are the liquid and particle densities respectively.

$$\mathrm{F_{CM}} = \frac{\left(\varepsilon_p^* - \varepsilon_m^*\right)}{\left(\varepsilon_p^* + 2\,\varepsilon_m^*\right)} \quad (5)$$

where p and m are subscripts corresponding to particle and medium respectively, and ε^* is the complex dielectric permittivity given by:

$$\varepsilon^* = \varepsilon_0\varepsilon - j\,\sigma/\omega \quad (6)$$

where ε is the relative effective permittivity, is the effective conductivity, ω is the angular frequency of the applied field and the symbol $j=\sqrt{-1}$ signifies that the dielectric displacement current leads the conduction current by a phase angle of 90°.

Equation 2 shows that the force induced by the travelling wave $\mathbf{F}_{TWD}$, see equation 7, (Huang, 1993), is counteracted by the viscous drag force $\mathbf{F}_v$, see equation 8, and it permits the establishment of the particle displacement velocity inside the medium.

$$\mathbf{F}_{TWD}=\frac{-4\pi\varepsilon_0\varepsilon_m r^3 \mathrm{Im}[\mathrm{F_{CM}}]\mathbf{E}^2}{\lambda} \quad (7)$$

where λ is the wavelength of the travelling field of value equal to the repetitive distance between electrodes of the same phase and $\mathrm{Im}[F_{CM}]$ is the imaginary part of the Clausius-Mosotti factor.

$$\mathbf{F}_v = 6\pi\eta rv \quad (8)$$

where is the dynamic viscosity and v is the particle displacement velocity.

A detailed analysis of equations 3 and 7 indicates that the direction of $\mathbf{F}_{DEP}$ and $\mathbf{F}_{TWD}$ is determined by the Clausius-Mosotti factor. Besides the strength and gradient of the electric field, the particle dynamics is controlled by the relationship between permittivities and conductivities of particles and medium.

3. METHODS AND MATERIALS

The TWD chamber consists of four aluminium electrodes wound in a square spiral. Electrodes are 5 μm width and their separation is 7 μm, which were grown in the metal layer of a CMOS process carried out at the Microelectronics National Centre in Barcelona, Spain. Spiral shapes pervade TWD applications because they permit the generation of a travelling wave over a large surface and can be fabricated in a single layer without any additional procedures.The power signal was supplied by a Hewlett Packard function generator and a custom-built circuit that offers four bipolar signals delayed 90° from each other. They were applied on the structure through manipulators of a Karl Suss test station.

Microsystems intended to handle biological particles are usually tested by means of polystyrene microspheres because their physical properties, as size and density, are quite similar to those of cells. In this case Fluoresbrite monodisperse microspheres of 6 μm in diameter and 2.5% of solids in water (Polysciences Europe GmbH), were used as test particles. They were resuspended in distilled water in a ratio of 10 parts of water to 1 of particles in their original concentration. Before the solution was micropipetted onto the electrodes surface it was sonicated for three minutes, which is helpful to keep microspheres in their monodisperse state.

The particle behaviour was observed through a Karl Zeiss stereomicroscope with a Sony camera attached to it. It was recorded on a video-tape in order to be later analysed. As shown in Figure 3, the experimental set-up was located onto an anti-vibration table to avoid the interference of external oscillations.

4. SIMULATIONS

Special care has been devoted to the estimation of the electric-field distribution. In order to compare DEP and TWD forces with the drag effect of the fluid motion arising from inhomogeneities in the medium triggered by thermal gradients (i.e. electrohydrodynamic phenomena), the thermal behaviour and the flow pattern were also assessed. The effects arising from electrochemical effects were neglected.

A two-dimensional (2-D) reduced model taking into account symmetries, periodicity, field shape and the appropriate boundary conditions over the central part of one spiral arm, was set up to assess the average electric field distribution over the

Furthermore, a 2-D axisymmetrical model with the Joule heat generation as thermal load was employed to obtain the thermal flux and gradient (TG) distributions in the structure. A transient simulation established that despite the final temperature distribution not being achieved until after about 10^2 seconds, depending on the precise shape and final mounting of the device, the TGs are stabilised in a neighbourhood of the electrodes in less than a second see Figure 4.

This is a pertinent remark because electrohydrodynamic (EHD) effects are only dependent on TGs and not on the temperature distribution. In other words, the dependence on the temperature variations, or thermal gradients, along the structure instead of the temperature itself is advantageous because it reduces the computation time as a result of the transient behaviour of TGs which stabilise faster than temperature.

The fluid motion profile was computed applying the electrostrictive forces per unit volume, whose formal expression was worked out by Ramos et al., 1998. These forces depend on the permittivity and conductivity of the suspension and on the amplitude and frequency of the applied signal. The fluid motion velocity scales like the fourth power of the applied signal amplitude because the EHD force also scales in this way. Such a scaling law allows us to take a quick look at the fluid velocity in the structure by solving the model only once for any value of the applied signal.

For an electrode width and separation of 20 μm (our numerical study case), and with V = 1 volt, typical fluid velocities of around 0.025 μm s^{-1} are obtained see Figure 5, which are completely negligible compared to the usual particle velocity values. If the voltage rises to 5 volts, common fluid velocities increase up to 16 m s^{-1}, which in many cases may be important when compared with that of the particle "free-fall" sedimentation velocity. In this case, the particle may be dragged by the fluid stream or its velocity can be slowed down, depending on whether the particle moves in the same direction as or in the opposite direction to the fluid.

Furthermore, if the driven voltage is set at 10 volts, the liquid velocity will be around 250 μm s^{-1}, which cannot be ignored. As can be seen, increasing the supplied voltage in a moderate way will cause a dramatic effect on the microdevice fluid motion pattern. In fact, velocities as high as those described in the last case will largely dominate the particle motion behaviour.

5. RESULTS AND DISCUSSION

When the power supply was applied, it was observed that particles placed over the central part of the arms of the spiral travelled towards or away from the centre of the structure, depending on the arm where the particles were placed. Inverting the signal supply sequence causes the particles' motion also to be inverted. The average motion velocity was about 120 μm s^{-1}, see Figure 6. When the driving voltage was raised to ± 6.5 V, the average motion velocity went to 150μm s^{-1}, while the other particle motion characteristics remained unaltered.

Particles near the diagonal follow a parabolic path: first they go to the centre and, when they cross the diagonal, they go far away. This behaviour may be explained because the spiral corners have the greatest electrical field gradients on the structure and a particle moving near them will suddenly change its direction. Besides motion, another visible effect is the particle cluster formation, which follows a similar kinematic behaviour to that of single particles.

At first glance such a linear motion of polystyrene microbeads could be understood as due to travelling wave dielectrophoresis (TWD). However, a careful review of the Clausius-Mossotti factor for latex microspheres suspended in de-ionised water reveals that at 190 kHz (the test frequency), particles should remain attached to the electrode edges as a result of a positive vslue in $\mathbf{F}_{DEP}$, but they did not! It was evident that there were other unconsidered effects which gave rise to the particle motion instead of the primarily studied dielectrophoretic force acting on the particle. Indeed, such a motion actually results as a consequence of the hydrodynamic viscous drag force affecting the particle, originated by the electrohydrodynamic (EHD) effects.

In fact, this observation led us to perform the numerical analysis described in section 4. This work showed that at low frequencies the fluid motion around the electrode corners consisted of a couple of whirlpools rotating in opposite directions while a continuous stream is developed over them, following the direction of the travelling-wave electric field applied, as shown in figure 5. Thus, if the voltage amplitude is high enough, particles can be dragged away by the fluid stream.

It should be remarked that, despite the huge range of applications, until now the theoretical and numerical studies of TWD have concentrated on the electric field and dielectrophoretic force distributions (Wang et al., 1994; Hughes et al., 1996). On the other hand, the lack of calculation taking into account the influence of other related phenomena, such as EHD, is noticeable. However, as shown in practice, the influence of EHD phenomena has to be considered, especially when working with media of high conductivities and high applied voltages, because they can influence or even dominate the particle motion behaviour in microstructures intended not only for TWD but also for cDEP applications.

5. CONCLUSIONS

In practice, linear motion of polystyrene microbeads of 6 m in diameter could be experimentally observed, as a consequence of a travelling wave of electric field generated over the square spiral microarray. At first glance, such results could be understood as due to TWD, but actually they correspond to particle motion as a result of EHD effects. In fact, this observation led us to perform the numerical analysis mentioned above. This work showed that the fluid flow motion around the electrode corners consists of a couple of whirlpools rotating in opposite directions, and a continuous stream is developed over them following the direction of the travelling-wave electric field applied. If the voltage amplitude is high enough, particles can be dragged away by the fluid stream. In other words, the numerical and practical results indicate that the influence of EHD phenomena has to be considered, especially when working with media of high conductivities and high voltages applied.

From a physical point of view, this research was mainly dedicated to TWD effects, as well as to the EHD phenomena that may alter or even control particle behaviour in the presence of travelling electric fields. It should be remarked that usually the theoretical and numerical studies of TWD have concentrated on the electric field and DEP force distributions, and the lack of calculation taking into account the influence of other related phenomena, such as electrohydrodynamic (EHD) phenomena, is noticeable. Of course, to design much more reliable and controllable devices based on TWD, the influence of EHD phenomena has to be considered.

Finally, motion of polystyrene microspheres on a CMOS microstructure was successfully experimentally verified. It should motivate the development of new CMOS microtools to perform handling, sorting, separation or characterisation of particles.

The main advantage of a device manufactured in CMOS technology is that active control circuitry required to develop a true microsystem-on-a-chip structure may be integrated onto it.

REFERENCES

Figeys, D. and Pinto, D. (2000). Anal. Chem. **72** 330a.

Fuhr, G., Arnold, W., Hagedorn, R., Müller, T., Benecke, W., Wagner, B. and Zimmermann, U. (1992). Biochem. Biophys. Acta **1108** p.p. 215.

Goater, A., Burt, J.P.H. and Pethig, J. (1997). Phys. D: Appl. Phys. **30** L65.

Huang, Y., Wang, X.B., Tame, J.A. and Pethig, R. (1993). J. Phys. D: Appl. Phys. 26 p.p. 1528.

Hughes, M.P., Wang, X.B., Becker, F.F., Gascoyne, P.R.C. and Pethig, R. (1994). J. Phys. D: Appl. Phys. **27** p.p. 1564.

Hughes, M.P., Pethig, R. and Wang, X.B. (1996). J. Phys. D: Appl. Phys. 29 p.p. 474.

Hughes, M. (2003). IEEE Med. and Biol. Mag. **22** p.p. 32.

Pohl, H. A. (1951) Appl. Phys. **22** p.p. 869.

Pohl, H.A. (1978). Dielectrophoresis: The behavior of neutral matter in nonuniform electric fields. (Cambridge University Press, London. p.p. 115.

Ramos, A., Morgan, H., Green, N.G. and Castellanos, A. (1998). J. of Phys. D: Appl. Phys. 31 p.p. 2338.

Talary, M.S., Burt, J.P.H., Tame, A. and Pethig, R. (1996) J. Phys. D: Appl. Phys. 29 p.p. 2198.

Wang, X.B., Huang, Y., Becker, F.F. and Gascoyne, P.R.C. (1994). J. Phys. D: Appl. Phys. 27 p.p. 1571.

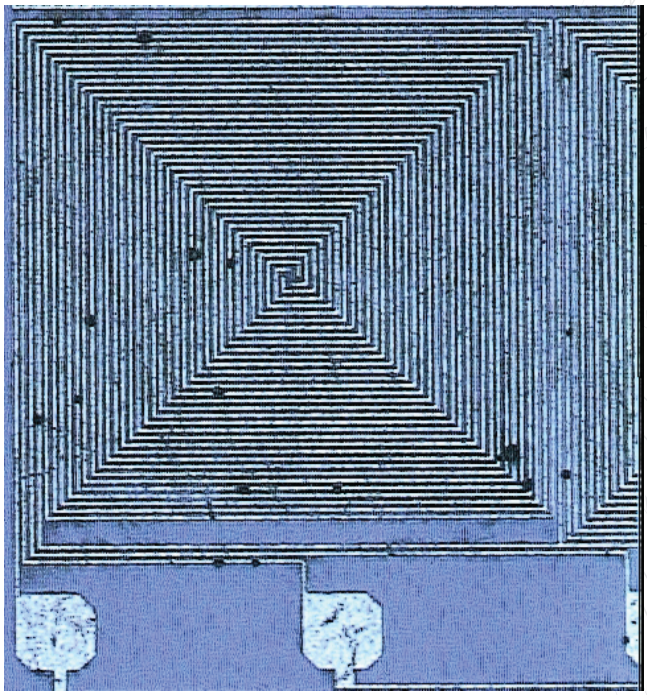

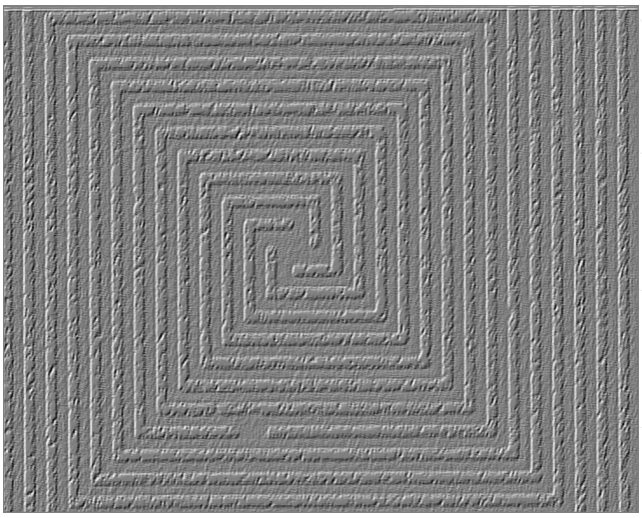

Figure 1.

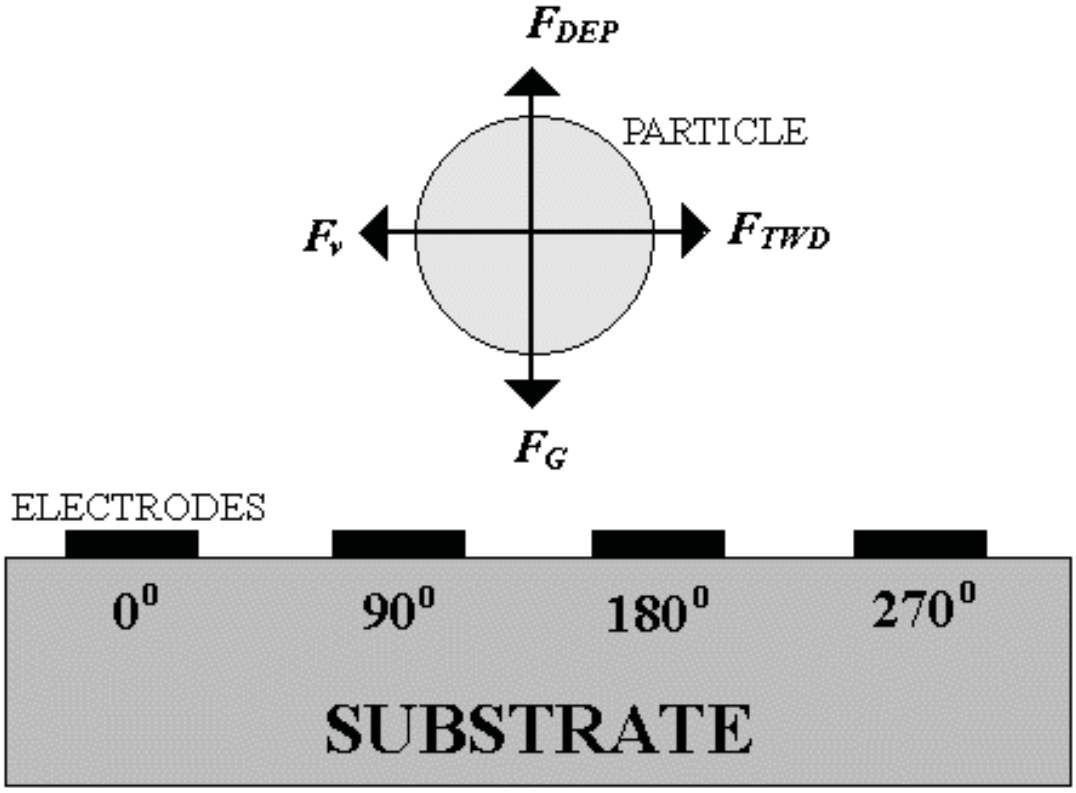

Figure 2.

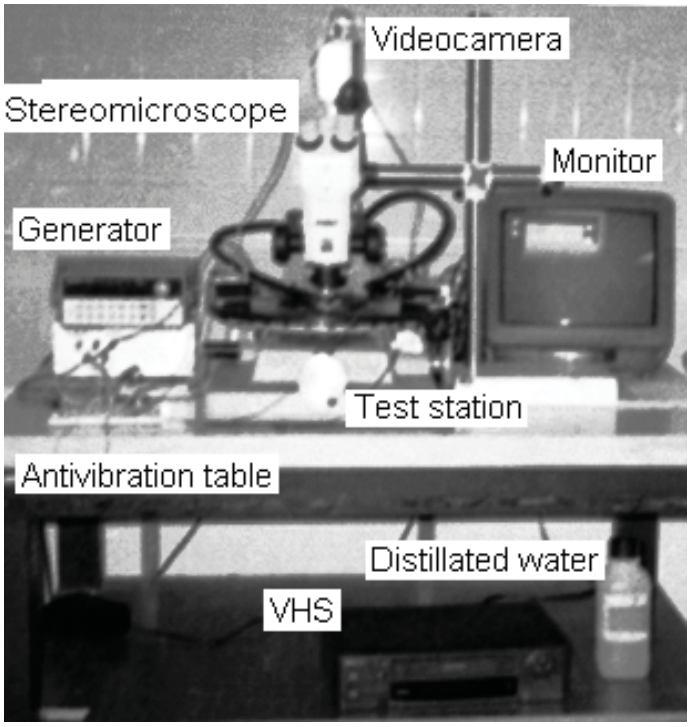

Figure 3.

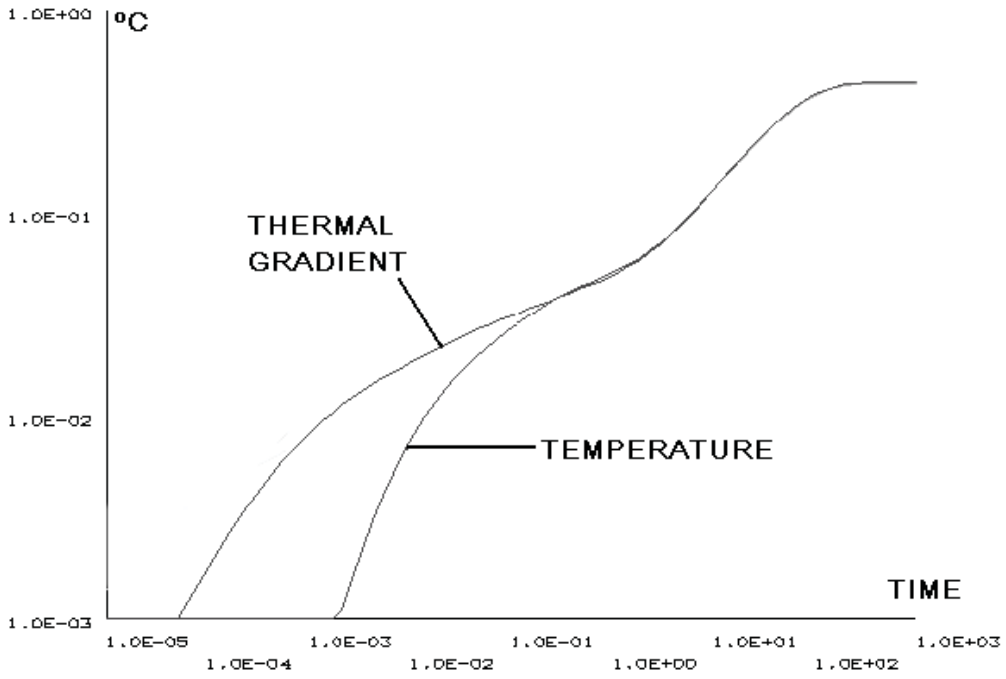

Figure 4.

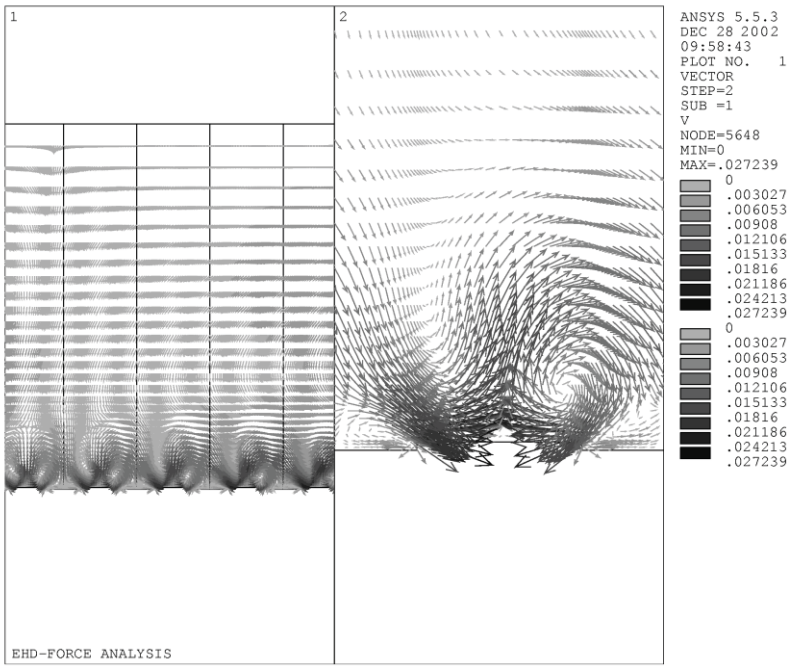

Figure 5.

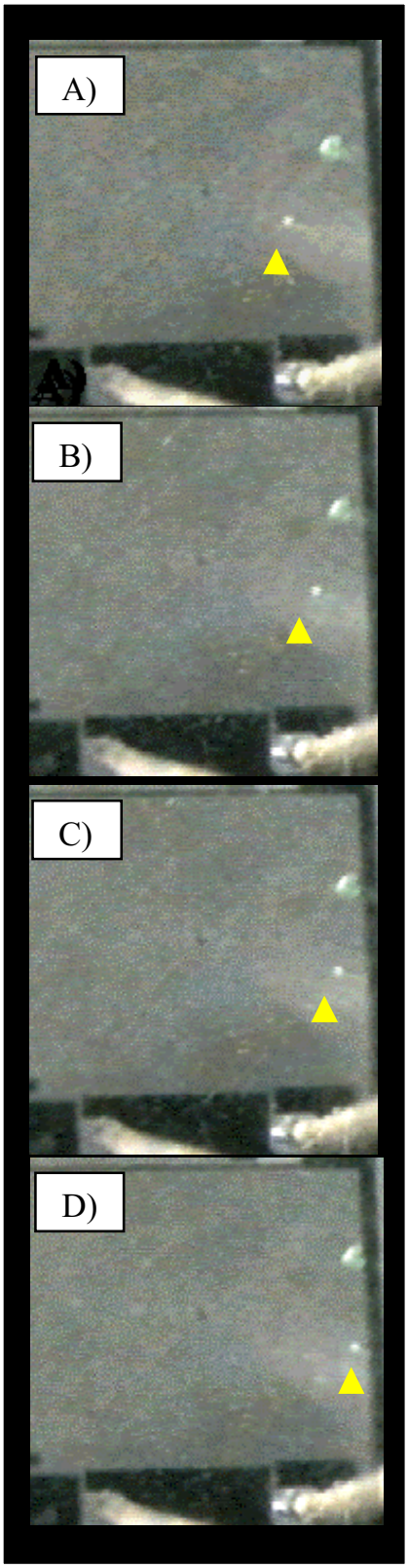

Figure 6.

Captions:

Figure 1. On the top there is a view of the four-meandering microelectrodes with a side length of 850 m. On the bottom the central microelectrode region is shown. The characteristic track width is 5 m.

Figure 2. Equilibrium force balance on a particle placed over the spiral symmetry axes. Electrodes are driven by four square-bipolar signals phased 90 apart.

Figure 3. Experimental set-up. Apparatus are placed on an anti-vibration table.

Figure 4. Microstructure transient thermal response. It takes about 10^2 sec. for T to stabilise, but for the gradients 1 sec. may be enough.

Figure 5. This figure shows the fluid motion behaviour at a frequency:of 100 kHz. On the left-side a few electrode domains are shown, while on the right-side ones a zoom of the neighbourhood of an electrode is represented. The applied voltage was 1 volt in a liquid of $_1$= 0.01 S m^{-1} and $_1$= 80. Velocity value is given in m s^{-1}.

Figure 6. Movement sequence of particle clusters over one of the spiral arms. The applied voltage was 4.5 V at 190 KHz with a solution conductivity of 1.26 mS m^{-1}. Frames were captured every 0.5 sec.